

1 **HYDRAULIC AND MECHANICAL PROPERTIES OF COMPACTED**
2 **BENTONITE AFTER 18 YEARS IN BARRIER CONDITIONS**

3 MARÍA VICTORIA VILLAR *, RUBÉN JAVIER IGLESIAS, CARLOS GUTIÉRREZ-ÁLVAREZ, BEATRIZ CARBONELL

4 Centro de Investigaciones Energéticas, Medioambientales y Tecnológicas (CIEMAT), Madrid, Spain
5

6 **Abstract**

7 The FEBEX “in situ” test was performed at an underground laboratory in Grimsel
8 (Switzerland) with the aim of studying the behaviour of components in the near-field of a
9 nuclear waste repository. A gallery of 2.3 m in diameter was excavated through the granite
10 and two heaters, simulating the thermal effect of the wastes, were placed inside, surrounded
11 by a barrier of highly-compacted bentonite blocks. In 2015, after 18 years of operation, the
12 experiment was dismantled. Some of the bentonite samples taken were tested in the laboratory
13 to characterize, among others, their physical state and determine their permeability and
14 swelling capacity.

15 There were significant changes in water content and dry density across the bentonite barrier:
16 their distribution was radial around the axis of the gallery, with the water content decreasing
17 from the granite towards the axis of the gallery and the dry density following the inverse
18 pattern.

19 The swelling capacity of the samples was related to their position in the barrier. In the
20 internal, drier part of the barrier an increase of the swelling capacity with respect to the
21 reference bentonite was detected, whereas the samples from the external part swelled less than
22 expected. This was attributed to the different salinity of the samples. The hydraulic
23 conductivity was mainly related to the dry density of the samples and decreased with respect
24 to the reference bentonite. This decrease was not related to the position of the samples and

25 could be related to the microstructural reorganisation of the bentonite during the 18-year
26 operation –which brought about an average decrease in the pore size– and to the low
27 hydraulic gradients applied to determine the permeability of the samples retrieved.

28 **1. Introduction**

29 The aim of the FEBEX project (Full-scale Engineered Barriers Experiment) was to study the
30 behaviour of components in the near-field of a repository in crystalline rock according to the
31 Spanish reference concept for geological disposal of nuclear waste. As part of this project an
32 “in situ” test, under natural conditions and at full scale, was performed at the Grimsel Test
33 Site (Switzerland), an underground laboratory managed by NAGRA (the Swiss agency for
34 nuclear waste management). A gallery of 2.3 m in diameter was excavated through the granite
35 and two heaters simulating the thermal effect of the wastes –with dimensions and weights
36 analogous to those of the real canisters– were placed inside a steel liner installed
37 concentrically with the gallery and surrounded by a barrier of highly-compacted bentonite
38 blocks. The external surface temperature of the heaters was 100°C and the bentonite barrier
39 was naturally hydrated by the granitic groundwater (ENRESA, 2006).

40 The heating stage of the in situ test began on February 1997. After five years of uninterrupted
41 heating at constant temperature, the heater closer to the gallery entrance (heater #1) was
42 switched off. In the following months this heater and all the bentonite and instruments
43 preceding and surrounding it were extracted. A large number of bentonite samples were also
44 taken for analysis in different laboratories (Villar et al. 2006). The remaining part of the
45 experiment was sealed with a new shotcrete plug and a second operational phase started with
46 the test configuration shown in Figure 1.

47 The clay barrier was built with compacted bentonite blocks arranged in vertical slices with
48 three concentric rings around the heaters (Figure 2). The thickness of the bentonite barrier in

49 the heater areas was 65 cm (distance from liner to granite). The blocks were obtained by
50 uniaxial compaction of the FEBEX clay with its hygroscopic water content (14%) at pressures
51 of between 40 and 45 MPa, what gave place to dry densities of 1.69-1.70 g/cm³. The initial
52 dry density of the blocks was selected by taking into account the probable volume of the
53 construction gaps and the need to have a barrier with an average dry density of 1.60 g/cm³
54 (ENRESA, 2006).

55 After 18 years of operation, the FEBEX Dismantling Project (FEBEX-DP) undertook the
56 dismantling of the experiment (García-Siñeriz et al. 2016). Heater #2 was switched off in
57 April 2015, the shotcrete plug was demolished and a month later the buffer removal and
58 sampling started. In particular, samples were taken to determine on site their water content
59 and dry density, with the aim of assessing the final state of the barrier. This was very much
60 affected by the processes to which the barrier had been subjected, namely hydration from the
61 granite and thermally-induced moisture redistribution. Some of the more remarkable
62 observations and common patterns were (Villar et al. 2016a):

- 63 – All the construction gaps between blocks had been sealed, both those among blocks of the
64 same section and the gaps between bentonite slices. The granite/bentonite contact was
65 also tight at all locations because of the swelling of the bentonite. This had already been
66 observed in the 2002 partial dismantling.
- 67 – The water content and dry density in every vertical section followed a radial distribution
68 around the axis of the gallery, with the water content decreasing from the granite towards
69 the axis of the gallery and the dry density following the inverse pattern. The water content
70 at all points in the barrier, even those close to the heater, was higher than the initial one,
71 i.e. greater than 14%. The water content and density gradients were steeper in those
72 sections affected by the heater.

73 Numerous bentonite samples were also taken and sent to CIEMAT's facilities. The sampling
74 took place in vertical sections normal to the axis of the tunnel –corresponding to original
75 block slices (Figure 1)–, and in each section several samples, mostly whole blocks, were
76 taken (Figure 2). These samples were tested to characterize their physical state (dry density,
77 water content) and determine, among others, their hydraulic and mechanical properties, such
78 as permeability and swelling capacity (Villar et al. 2018).

79 The aim of the research reported here was to assess if the operation under repository
80 conditions implied irreversible changes on the main properties of the bentonite. For that, the
81 extensive database on the variation of these properties with different parameters (dry density,
82 water content, temperature, salinity) obtained over the last 20 years for the FEBEX bentonite
83 (e.g. Villar 2002, ENRESA 2006, Castellanos et al. 2008, Villar & Lloret 2008) has been
84 used. .

85 The same kind of analyses was done in the samples retrieved during the first dismantling in
86 2002 (Villar et al. 2006, Villar & Lloret 2007). Some of the conclusions reached in those
87 works related to the hydro-mechanical properties of the materials were:

- 88 – The hydraulic conductivity of the samples retrieved after 5 years of operation was clearly
89 related to dry density and the latter in turn was related to the position of the sample in the
90 barrier. The values of hydraulic conductivity measured for the samples of lower density
91 (more hydrated) were in the order of those expected for untreated bentonite, but for
92 samples of higher densities there was a large dispersion in the values obtained without any
93 clear tendency.
- 94 – The final swelling strains upon saturation under a low vertical load of the samples
95 retrieved after 5 years of operation were in the order of those expected for untreated
96 FEBEX bentonite compacted at the same dry density with the same water content.

97 Up to the whole dismantling of the FEBEX in situ test, no bentonite subjected to repository
98 conditions for such a long period of time had ever been studied. Nevertheless, other shorter
99 full-scale experiments reproducing different disposal concepts have been dismantled and
100 analysed in a similar way. Some of the older ones were discussed in Villar & Lloret (2007). In
101 the last decade, several experiments in which compacted bentonite was used as engineered
102 barrier were dismantled at the Äspö Hard Rock Laboratory in Sweden – also excavated in
103 crystalline rock–, and the conclusions regarding the HM analyses performed on the samples
104 retrieved can be summarised as follows:

- 105 – The “Long Term Tests of Buffer Material” (LOT) included seven test parcels in which
106 MX-80 bentonite was used as barrier material. Two pilot parcels (A1 and S1) were
107 dismantled and analysed after 1 year operation (Karnland et al. 2000), an additional parcel
108 (A0) was exposed to adverse conditions for 1.5 years (Karnland et al. 2011), and a
109 medium-term parcel (A2) was dismantled after 6 years operation (Karnland et al. 2009).
110 No significant changes in the swelling pressure and hydraulic conductivity were detected
111 in any of the parcels, although some trimmed samples showed a decrease in hydraulic
112 conductivity with respect to the reference material not related to the thermal gradient.
- 113 – The “Alternative Buffer Material” (ABM) consisted of three packages where eleven
114 different clays were tested as buffers. Package 1 and 2 were dismantled after 2 and 6.5
115 years, respectively. After 2 years (one of them with the heater set to 130°C) no difference
116 was seen in hydraulic conductivity between samples from the field experiment and the
117 corresponding reference materials. However, a significant decrease in swelling pressure
118 was seen for two of the bentonites used. The largest deviation was noticed on samples
119 from the warmest part during the experiment. The proposed explanation for this decrease
120 in swelling pressure was the significant redistribution of cations in the test package, which
121 could have influenced the physical properties of the clays (Svensson et al. 2011).

- 122 – The “Prototype Repository” consisted of six deposition holes divided into two sections
123 (sections I and II, containing four and two holes, respectively). Each deposition hole had a
124 full-scale buffer of compacted bentonite (MX-80) surrounding a copper canister equipped
125 with heaters. Section II was dismantled after 8 years of hydrothermal exposure, and it was
126 found that the degree of saturation was not homogeneous in any of the two buffers
127 (Olsson et al. 2013). No large variations were observed in the swelling pressure of the
128 field-exposed bentonite with respect to the reference bentonite, however the field-exposed
129 bentonite had lower hydraulic conductivity than the reference specimens, especially at
130 high densities. These changes were not related to the position of the samples in the buffer,
- 131 – The “Canister Retrieval Test” (CRT) experiment consisted of a cylindrical deposition hole
132 hosting a canister encapsulated in clay buffer (MX-80). After 5 years operation the
133 experiment was shut down and dismantled in 2006. When compared to reference material
134 properties the hydro-mechanical analyses of the buffer samples showed no significant
135 change in swelling pressure, although there was a slight decrease in hydraulic
136 conductivity for the higher density samples. No coupling was found between these
137 changes in the hydro-mechanical properties and the montmorillonite characteristics
138 (Dueck et al. 2011a, b).

139 **2. Material**

140 The bentonite used to construct the engineered barrier was the FEBEX, extracted from the
141 Cortijo de Archidona deposit in SE Spain. The physico-chemical properties of the FEBEX
142 bentonite, as well as its most relevant thermo-hydro-mechanical and geochemical
143 characteristics were summarised in ENRESA (2006).

144 The montmorillonite content of the FEBEX bentonite is above 90 wt.% (92±3 %). The
145 smectitic phases are actually made up of a smectite-illite mixed layer, with 10-15 wt.% of

146 illite layers. Besides, the bentonite contains variable quantities of quartz (2 ± 1 wt.%),
147 plagioclase (3 ± 1 wt.%), K-felspar (traces), calcite (1 ± 0.5 wt.%), and cristobalite-trydimite
148 (2 ± 1 wt.%). The cation exchange capacity of the smectite is 102 ± 4 meq/100g, the main
149 exchangeable cations being calcium (35 ± 2 meq/100g), magnesium (31 ± 3 meq/100g) and
150 sodium (27 ± 1 meq/100g). The predominant soluble ions are chloride, sulphate, bicarbonate
151 and sodium.

152 The liquid limit of the bentonite is 102 ± 4 %, the plastic limit 53 ± 3 %, the density of the solid
153 particles 2.70 ± 0.04 g/cm³, and 67 ± 3 % of particles are smaller than 2 μ m. The hygroscopic
154 water content in equilibrium with the laboratory atmosphere is 13.7 ± 1.3 %. The external
155 specific surface area is 32 ± 3 m²/g and the total specific surface area is about 725 m²/g.

156 Based on numerous swelling under load tests performed with the FEBEX bentonite
157 compacted to different initial dry densities (ρ_{d0} , g/cm³) with different water contents (w_0 , %),
158 an empirical relation predicting the final swelling strain (ε , %) after saturation with deionised
159 water under vertical load of 0.5 MPa was determined (Villar & Lloret 2008):

$$160 \quad \varepsilon = (37.48 \rho_{d0} - 50.43) \ln w_0 - 154 \rho_{d0} + 204.24 \quad [1]$$

161 The saturated hydraulic conductivity of compacted bentonite samples is exponentially related
162 to their dry density. An empirical relationship for the reference FEBEX bentonite relating
163 hydraulic conductivity (k_w , m/s) to dry density (ρ_d , g/cm³) was obtained for samples
164 compacted to dry densities above 1.47 g/cm³ and permeated with deionised water (Villar
165 2002):

$$166 \quad \log k_w = -2.96 \rho_d - 8.58 \quad [2]$$

167 The variation in the experimental values with respect to this fitting is on average of 30%,
168 which should be evaluated taking into account that the values of permeability are of the order

169 10^{-14} m/s. The hydraulic gradients applied in these determinations were on average of 15200
170 m/m.

171 **3. Methodology**

172 CIEMAT received samples conveniently preserved on site and the packing was only removed
173 just before subsampling in the laboratory. Subsampling from the blocks was mostly
174 performed by drilling with crowns of different diameters.

175 Samples were taken specifically to determine the water content and dry density of the blocks
176 at two or three positions along the radius of the block, The gravimetric water content (w) is
177 defined as the ratio between the mass of water and the mass of dry solid expressed as a
178 percentage. The mass of dry soil was determined by oven drying at 110°C for 48 h. Dry
179 density (ρ_d) is defined as the ratio between the mass of the dry sample and the volume
180 occupied by it prior to drying. The volume of the specimens was determined by immersing
181 them in a recipient containing mercury and by weighing the mercury displaced (applying
182 Archimedes' principle and considering a specific weight for the mercury of 13.6 g/cm³). The
183 same samples whose volumes had been determined were used for the water content
184 determination.

185 For the hydro-mechanical tests the samples were drilled at two locations (subsamples 1 and 2,
186 being 1 the closer to the granite) in each block using a crown of internal diameter 5.7 cm.
187 They were later adapted to the diameter of the cell rings with a cylindrical cutter and finally
188 pushed inside the stainless steel cell rings. Care was taken during the process to preserve the
189 original moisture and density of the samples. The identification of each sample was given by
190 the name of the block from which it was drilled (see Figure 2) and the number of the
191 subsample (1 or 2).

192 **Swelling under load tests**

193 The saturation (or swelling) under load test makes it possible to determine the swelling
194 capacity of the soil when it saturates under a previously established vertical pressure while it
195 is kept laterally confined. The tests were performed in standard oedometers following
196 approximately ASTM D 4546-03 Method A. The samples obtained by drilling and trimming
197 had diameters between 3.6 and 5.0 cm and heights between 1.3 and 1.7 cm. Once in the
198 oedometer, a vertical pressure of 0.5 MPa was applied to the samples. After stabilisation of
199 the deformation, the samples were saturated with deionised water at atmospheric pressure
200 from the bottom porous plate. The swelling strain experienced by the specimens upon
201 saturation was recorded as a function of time by linear strain transducers (LSCT) until
202 stabilisation. During most of the tests, the electrical conductivity of the water in the
203 oedometer was measured periodically with an electrical conductivity meter, which was
204 submerged in the oedometer water every time the cell was refilled with deionised water to
205 keep the water level in the cell approximately constant.

206 The ratio between the final length increase undergone by the sample in equilibrium with the
207 load applied and its initial length gives the strain value of the material on saturation, the
208 negative values indicating swelling strains. The final result is, therefore, the percentage of
209 strain of a sample of given initial dry density and water content on saturation under a fixed
210 load. The final strain is used to compute the final dry density of the specimens, which is
211 assessed by measurement of the actual specimen dimensions upon dismantling. On
212 completion of the tests, the water content of the specimen was determined by oven drying at
213 110 °C for 48 hours. The tests were performed at laboratory temperature.

214 **Hydraulic conductivity**

215 The hydraulic conductivity was measured according to a constant-head method developed at
216 CIEMAT for expansive soils, in which the specimens are tested in stainless steel cells that
217 guarantee the constant volume of the samples during the whole measuring process (Villar
218 2002). The samples obtained by drilling and trimming were confined in rigid cells of internal
219 diameter 5.0 cm. The height of the samples –which was kept constant during the tests– was
220 between 2.2 and 2.8 cm and filter papers and porous stones were placed on their top and
221 bottom. The samples were saturated from both faces with deionised water injected at a
222 pressure of 0.6 MPa over the necessary time period. This was checked by measuring the water
223 intake until stabilisation. The saturation under pressure allowed the dissolution of the air
224 contained in the pores, which volume was not expected to be large because of the high initial
225 degree of saturation of most samples (>83% in all of them). Once the sample was saturated a
226 hydraulic gradient was applied across it by increasing the pressure at the bottom of the cell,
227 while the downstream pressure on top was maintained lower. The complete saturation of the
228 sample and associated swelling guaranteed perfect contact with the walls of the cell,
229 preventing the flow of water between these and the sample. The hydraulic gradients applied in
230 these tests were of between 1600 and 11700 m/m. The water volume passing through the
231 sample was measured online with pressure/volume controllers resolving 1 kPa and 1 mm³.
232 The tests run over a time period sufficient to determine that the volume of water passing
233 through the specimen was linear and stable with time for a given hydraulic gradient.
234 Hydraulic conductivity was then calculated by applying Darcy's law for flow in porous
235 media.

236 Two or three different hydraulic gradients were applied to each sample and the tests were
237 performed at room temperature. At the end of the tests, the samples were weighed, measured
238 and oven-dried at 110°C for 48 h to check their final water content and dry density.

239 **4. Results**

240 The water content of the samples tested in the laboratory decreased from the granite towards
241 the inner part of the barrier in all the sampling sections, whereas the dry density increased. In
242 particular, in the sections around the heater analysed in this work the water content and dry
243 density gradients were steep and linear, with values between 18 and 28% for the water content
244 and 1.54 and 1.65 g/cm³ for the dry density. In the three radii sampled in every section the
245 changes were similar, which confirms the radial distribution pattern. The water content and
246 dry density values obtained in the laboratory agreed very well with those obtained on site
247 (Figure 3), what suggests that the packing and transport conditions were the appropriate to
248 keep the *in situ* state of the blocks even several months after their retrieval.

249 The broad range of values found in the laboratory for both variables means that the initial
250 conditions of the samples tested to determine their hydro-mechanical properties were very
251 different and this had an impact on the results obtained.

252 **Swelling under load tests**

253 The swelling capacity was tested in 20 samples taken at different distances from the heater.
254 The process of sample preparation, drilling and trimming to make the specimen fit into the
255 cell ring, meant in most cases a decrease of the density of the specimen in the oedometer ring
256 with respect to the dry density of the block from which they were obtained (the one shown in
257 Figure 3).

258 The evolution of the vertical strain during the swelling tests in samples from section S47 is
259 shown in Figure 4. The samples closer to the gallery wall tended to have higher initial water
260 content and lower initial dry density, in agreement with the values of the blocks from which
261 they were obtained (Figure 3). The swelling capacity is related to both, increasing with initial
262 dry density and decreasing with initial water content (Eq. 1). For this reason the final strain of

263 the samples closer to the heater tended to be higher. It also took longer for the deformation of
264 these samples to stabilise. An exception to this general observation is sample BB47-4-2,
265 which despite belonging to the external ring of the barrier swelled considerably. The most
266 likely reason is its high initial dry density (1.59 g/cm^3), which does not correspond to its
267 position in the barrier (Figure 3, right) and was probably caused by unintended compaction
268 during specimen preparation for the swelling test. The final vertical strain recorded in all the
269 tests is shown in Figure 5, where the trend for finding higher vertical strains in the samples
270 closest to the heater is confirmed, since the samples closer to the gallery wall tended to have
271 higher initial water content and lower initial dry density. Indeed the original dry density of the
272 blocks from which the samples were trimmed was modified during trimming and sample
273 preparation, and that is the reason why the dry densities indicated in Figure 5 do not show a
274 straightforward increase towards the axis of the gallery. Nevertheless, the water content did
275 decrease for each sampling section towards the axis of the gallery (because it was barely
276 affected by sample preparation) and the combination of lower water content and (mostly)
277 higher dry density, made the swelling capacity increase on average towards the internal part
278 of the barrier.

279 **Hydraulic conductivity**

280 The hydraulic conductivity was measured in specimens drilled from blocks after they were
281 saturated with deionised water for periods of time of between 13 and 86 days. Although many
282 samples had a high initial degree of saturation, they took water because, once in the cell, their
283 density decreased with respect to the original value, due to the filling of some irregularities
284 that could have been created during trimming. In fact, there was a decrease in dry density of
285 the samples tested in the permeability cells with respect to that of the blocks from which they
286 were trimmed (the one shown in Figure 3), because of the sample preparation process
287 described above.

288 After saturation, hydraulic gradients of between 1600 and 11700 m/m were applied to the
289 samples and kept until the outflow rate was constant. Afterwards, the hydraulic gradient was
290 changed and kept again until constant outflow rate. In some cases a third hydraulic gradient
291 was applied. The whole measuring process took between 28 and 106 days. For the first
292 samples tested, lower hydraulic gradients were applied (below 4000). Some of the values
293 obtained have been plotted as a function of the hydraulic gradient applied in Figure 6.
294 Although there is not a clear relationship between hydraulic conductivity and gradient, the
295 lowest permeabilities were measured when hydraulic gradients below 5000 were used.

296 The results are plotted in Figure 7 as a function of the position in the barrier. The dry density
297 of each sample, computed from the bentonite dry mass and the internal volume of the cell, is
298 also indicated in the Figure. As a general rule the hydraulic conductivity of bentonite is
299 mainly related to dry density (Eq. 2) and the latter in turn should be related to the position of
300 the block in the barrier (Figure 3). Consistently with this, the overall trend in section S47 is
301 for the hydraulic conductivity to decrease towards the heater, where the densities should be
302 higher, whereas for section S53 there is not a clear dependence of hydraulic conductivity on
303 the position of the sample inside the barrier. This is probably because the two samples drilled
304 from the middle block of the barrier in section S53 had –as a consequence of trimming–
305 higher dry density than those in the internal and external blocks, and consequently lower
306 hydraulic conductivity.

307 The hydraulic conductivity values have been plotted in Figure 8 as a function of the dry
308 density inside the permeability cell. The decrease of hydraulic conductivity with dry density
309 is highlighted in the Figure. The fact that the decrease in dry density of the samples prepared
310 for the permeability tests with respect to the original density of the blocks was not of the same
311 magnitude for all the samples (as observed in section S53) might be the reason why the
312 relation between hydraulic conductivity and distance to the axis was not straightforward.

313 The empirical relationship for the reference FEBEX bentonite relating hydraulic conductivity
314 to dry density obtained for samples compacted to dry densities above 1.47 g/cm^3 and
315 permeated with deionised water (Eq. 2) is also shown in Figure 8, along with its range of
316 variation. When comparing these values to those expected for untreated FEBEX bentonite of
317 the same dry density, it is found that the values for the FEBEX-DP samples were below the
318 theoretical ones, in many cases even below the expected range of variation of this property for
319 FEBEX bentonite.

320 **5. Discussion**

321 When analysing the hydro-mechanical properties of the bentonite retrieved from the FEBEX
322 in situ test, the changes experienced by the bentonite during sampling on site and during
323 preparation of specimens in the laboratory have to be taken into account. Although the
324 samples were preserved carefully and their water content did not seem to have changed with
325 respect to that the samples had during operation, the stresses in the barrier (which at some
326 points were as high as 6 MPa during operation (Martínez et al. 2016) were released upon
327 dismantling, and this probably implied a decrease in the bentonite dry density. Additionally,
328 as it has been explained above, the preparation of specimens to fit the testing rings required
329 drilling and trimming, which caused a decrease in the final dry density of the samples tested
330 with respect to that of the bentonite blocks from which they were taken. The same observation
331 was made earlier in the samples from the partial dismantling of the FEBEX in situ test (Villar
332 & Lloret, 2007) and by other authors analysing samples retrieved from large-scale tests
333 (Karnland et al. 2009, 2011). This decrease was not in all the cases of the same magnitude,
334 since it depended on the sample conditions and on the operator.

335 Nevertheless, the aim of the determination of the hydraulic properties reported was to check if
336 they had irreversibly changed during operation with respect to those of the reference

337 bentonite. For this reason, the values obtained are compared in the following with those
338 expected under the same testing conditions for the reference FEBEX bentonite.

339 In order to evaluate the modification of the swelling capacity of the bentonite as a result of the
340 18-year operation, the final vertical strain measured has been compared with the theoretical
341 vertical strain of samples of the reference FEBEX bentonite of the same initial dry density
342 and water content saturated under the same conditions, i.e. same vertical load and kind of
343 water, since all these parameters affect the swelling capacity. Thus, the measured values and
344 the theoretical results obtained with Eq. 1 for each sample are plotted in Figure 9. On average
345 the vertical strains actually measured were lower than the theoretical ones (-10% vs. -12%).
346 The Figure includes also the distance to the gallery axis of each sample. Most samples from
347 the external, more saturated bentonite ring swelled less than expected, whereas the samples
348 from the inner, drier ring tended to swell as expected or more. This could be related to their
349 higher initial salinity, which would have triggered some additional osmotically-induced
350 swelling. The high salinity of the pore water of the samples close to the heater was confirmed
351 in the geochemical characterisation of samples retrieved from Grimsel performed by
352 Fernández et al. (2017). In this work the very low salinity (lower than the one for the
353 reference bentonite) of the samples from the external ring was also highlighted. The
354 explanation given to the salinity changes across the barrier is that the water coming from the
355 host rock dissolved soluble species and transported them towards the internal part of the
356 barrier, where they accumulated. Hence, there were differences in the initial salinity of the
357 samples tested in the oedometers. The electrical conductivity of the water in the oedometer
358 cells was measured during the tests. In the tests performed with samples from the inner ring
359 (the one closest to the heater), the electrical conductivity increased considerably during the
360 tests, which would indicate that the soluble salts in the bentonite were being dissolved by the
361 deionised water and transported outside the bentonite and into the water in the oedometer cell.

362 On the contrary, the electrical conductivity of the water in the oedometer cells in which
363 samples from the external ring, the one closest to the granite, were being tested barely
364 increased during the tests. As an example, Figure 10 shows the simultaneous evolution of
365 swelling strain and electrical conductivity of the water in the oedometer cell for two samples
366 of section S53, one of them obtained from the external bentonite ring (taken at 110 cm from
367 the gallery axis) and the other one from the internal ring (taken at 53 cm from the gallery
368 axis). Because of trimming, the initial dry density of these two specimens was similar, despite
369 the fact that the blocks from which they were obtained had considerably different densities.
370 The sample from the internal ring swelled more and for longer, with the electrical
371 conductivity of the water in the oedometer cell increasing considerably, particularly after 10
372 days, when most swelling had already been developed. This could imply that the osmotically-
373 induced part of swelling (indicated by the increase in electrical conductivity) was less
374 important and was not remarkable until the crystalline swelling had been completed.

375

376 The hydraulic conductivity values measured in the samples retrieved were clearly lower than
377 those expected for samples of untreated bentonite of the same dry density (Figure 8). In
378 particular, the samples tested using hydraulic gradients below 4000 m/m had hydraulic
379 conductivities clearly below those expected for the reference bentonite. On the contrary, the
380 samples tested with higher hydraulic gradients had higher hydraulic conductivities. The
381 determinations for the reference bentonite were performed applying hydraulic gradients on
382 average of 15200 m/m, i.e. higher than those used for the testing of the FEBEX-DP samples.
383 Back in 1976, Kharaka & Smalley pointed out the increase in hydraulic conductivity of
384 compacted clays with the increase in hydraulic pressure gradients. Dixon et al. (1999)
385 investigated the hydraulic conductivity of clays, among which bentonites, and found a
386 transitional gradient below which low flow rates were recorded whereas above them the

387 flows, and consequently permeabilities, were higher. A previous research analysing the effect
388 of hydraulic gradient on permeability of the FEBEX bentonite found that –in some cases– the
389 permeability tended to be slightly lower as the hydraulic gradient decreased (Villar & Gómez-
390 Espina 2009). Hence, it is considered that the lowest permeability values measured in the
391 present work can be a consequence of having used hydraulic gradients close to the critical
392 ones in some samples. The critical gradient, as defined by Olsen (1962), would be the
393 hydraulic gradient below which flow occurs but it is non-Darcian (i.e. the relationship
394 between flow and hydraulic gradient is not linear), because of the strong clay-water
395 interactions. The existence of threshold and critical hydraulic gradients for water flow in
396 bentonite has been taken into account to model the hydration of the clay barrier by Sánchez et
397 al. (2007).

398 Unlike what was observed in the swelling capacity tests, this decrease did not seem to be
399 related to the position of the samples in the barrier. The osmotic effect is ruled out on the
400 permeability samples, because during saturation the samples were confined and not able to
401 swell differently during the permeability measurement as it happened in the swelling capacity
402 tests.

403 There is also the possibility that, during the 18 years operation, the microstructure of the
404 bentonite experienced changes that could affect the water flow. It is known that saturation
405 involves a homogenisation of pore sizes towards the smaller sizes, and this makes the intrinsic
406 permeability of the bentonite decrease with the degree of saturation (Villar & Lloret, 2001).
407 Indeed this process took place during the saturation of the samples in the permeability cell,
408 and it certainly occurred also during saturation of the samples used to determine the
409 permeability of the reference bentonite. But it could have happened that over the 18 years of
410 saturation in the barrier the average pore size had become lower and more homogeneous, and
411 this would explain the lower hydraulic conductivity of the samples that were submitted to

412 barrier conditions. In fact, the pore size distribution of the retrieved samples obtained by
413 mercury intrusion porosimetry showed an increase in the percentage of pores smaller than 50
414 nm with respect to the reference bentonite. Also, the measurement of the basal spacing of
415 these samples by X-ray diffraction indicated that the interlayer distance between smectite
416 particles had increased from the initial value of 1.48 nm to values higher on average than 1.55
417 nm, as a consequence of the water content increase in the smectite interlayer (Villar et al.
418 2018). The modification of the FEBEX bentonite microstructure as a result of prolonged
419 hydration, with overall increase of the microstructural void ratio and of the proportion of
420 adsorbed, interlayer water, was also observed in the 12-year long thermo-hydraulic laboratory
421 tests reported by Villar et al. (2016b). These works concluded that the maturation of the
422 barrier would lead to a decrease in free water availability, since most water would eventually
423 enter the interlayer porosity, a process that has been also described under different testing
424 conditions by other authors (e.g. Karnland et al. 2006). The decrease in the average pore size
425 along with the decrease in free/adsorbed water ratio would make the permeability of the
426 material decrease over time, until equilibrium among pores and kinds of water is reached.
427 Interestingly, the analyses performed in samples retrieved from the large-scale tests
428 performed at the Äspö Hard Rock Laboratory summarised in the Introduction of this paper,
429 showed also in some cases a slight decrease in the hydraulic conductivity of the MX-80 buffer
430 with no spatial trend.

431 **6. Conclusions**

432 The FEBEX in situ test was a full-scale experiment performed under natural conditions to
433 reproduce the conditions of the engineered barrier system in an underground repository of
434 nuclear waste. The barrier around the heater simulating the waste container was composed of
435 FEBEX bentonite blocks and had an average dry density of 1.6 g/cm³. After 18 years of

436 operation under repository conditions, natural hydration from the granitic host rock and
437 heating from the heater, the heater was switched off and the experiment was dismantled.

438 This paper has presented the results of part of the hydro-mechanical characterisation of
439 bentonite samples taken during dismantling. The main objective of this work was assessing if
440 these properties had irreversibly changed as a consequence of the conditions during operation.
441 To this aim, the values for these properties obtained in the samples retrieved from Grimsel
442 were compared with those expected for the reference, untreated bentonite tested in the same
443 way.

444 The bentonite water content decreased from the external part of the barrier (close to the
445 granite) towards the internal part (i.e. the axis of the gallery) and the dry density followed the
446 inverse pattern. Consequently, the samples retrieved had very different water contents and dry
447 densities, both of which affect greatly the hydro-mechanical properties.

448 The preparation of specimens for the swelling capacity and hydraulic conductivity tests
449 caused some reduction in their dry density with respect to the original dry density of the
450 bentonite blocks. Since the evaluation of the change of these properties during operation was
451 done by comparing with untreated samples of the same dry density and water content, this
452 density decrease does not impair the conclusions obtained, but it has to be taken into account
453 that the permeability and swelling strain values measured do not correspond to those the
454 bentonite had in the barrier, where its dry density was higher and some boundary conditions
455 (water availability and salinity, stress state) were different.

456 The swelling capacity of the samples taken from the external ring of the barrier, i.e. those
457 more saturated, was lower than expected, whereas the samples from the inner ring of the
458 barrier, those closest to the heater, swelled in the range expected of even more. The reason for
459 these observations could be the different content in soluble salts of the samples depending on
460 their position in the barrier: the pore water of the samples closest to the granite had been

461 leached by the water coming from the host rock and moving inwards. On the contrary, the
462 salinity of the samples closest to the heater was much higher than the initial one because the
463 soluble species concentrated in this area. This salinity would have triggered some additional
464 osmotically-induced swelling, as the salts in the bentonite were dissolved and moved towards
465 the water in the oedometer cell, which was periodically refilled with deionised water. This
466 process did not take place in the reference bentonite or in the more saturated bentonite from
467 the external ring, because in both cases the salinity was lower. It has to be highlighted that
468 this is a process that took place because the samples were let swell under a low vertical stress
469 in a relatively large volume of water, but the same conditions are not to be encountered in the
470 barrier during operation.

471 The hydraulic conductivity of the samples retrieved was in the order of 10^{-14} m/s and mainly
472 related to the dry density of the samples, but overall it was lower than expected for the
473 untreated FEBEX bentonite. The fact that the hydraulic gradients applied in this work were
474 lower than those used to determine the hydraulic conductivity of the reference bentonite, and
475 in some cases close to the critical hydraulic gradient (i.e. the gradient below which flow is
476 non-Darcian as a result of the strong clay-water interactions), could have contributed to this
477 difference. Also, a decrease of the average pore size of the bentonite during the 18-year
478 operation and a decrease of the free/adsorbed water ratio, more drastic than the one to be
479 expected during the relatively short period of saturation that precedes the permeability
480 determination, could play a part in the decrease of hydraulic conductivity observed.

481 Despite the changes observed in the properties analysed with respect to those of the reference
482 bentonite, the performance of the barrier was very good, the permeability continued to be low
483 and the swelling capacity was very high and enough to fill all the construction gaps of the
484 barrier. The dry density and water content gradients observed in the barrier have a
485 repercussion on its hydro-mechanical properties, since most of them depend greatly on the

486 density and water content of the bentonite. This could lead to an inhomogeneous distribution
487 of swelling pressure and permeability in the barrier that should be taken into account when
488 modelling the barrier behaviour and evolution.

489 **Acknowledgements**

490 The FEBEX-DP Consortium (NAGRA, SKB, POSIVA, CIEMAT, KAERI) financed the
491 dismantling operation in 2015. The support of the responsible person of the Consortium, Dr.
492 Florian Kober, is greatly acknowledged. This work has been financed by the FEBEX-DP
493 consortium and through Annex XLII of the ENRESA-CIEMAT framework agreement.
494 Beatriz Carbonell was hired in the framework of the Spanish National System of Youth
495 Guarantee in R+D 2014, with financing of the European Social Fund and the Youth
496 Employment Initiative.

497

498 **7. References**

499 ASTM D4546-03. 2003. Standard Test Methods for One-dimensional swell or settlement
500 potential of cohesive soils. 7 pp.

501 Castellanos, E.; Villar, M.V.; Romero, E.; Lloret, A. & Gens, A. 2008. Chemical impact on
502 the hydro-mechanical behaviour of high-density FEBEX bentonite. *Physics and*
503 *Chemistry of the Earth* 33: S516-S526.

504 Dixon, D., Graham, J., Gray, M.N. 1999. Hydraulic conductivity of clays in confined tests
505 under low hydraulic gradients. *Canadian Geotechnical Journal* 36(5): 815-825.

506 Dueck A, Johannesson L-E, Kristensson O, Olsson S, 2011a. Report on hydro-mechanical
507 and chemical-mineralogical analyses of the bentonite buffer in Canister Retrieval Test.
508 Technical Report SKB TR-11-07, Svensk Kärnbränslehantering AB.

509 Dueck A, Johannesson L-E, Kristensson O, Olsson S, Sjöland A, 2011b. Hydro-mechanical
510 and chemical-mineralogical analyses of the bentonite buffer from a full-scale field

511 experiment simulating a high-level waste repository. *Clays and Clay Minerals* 59,
512 595–607.

513 ENRESA 2006. FEBEX Full-scale Engineered Barriers Experiment, Updated Final Report
514 1994-2004. Publicación Técnica ENRESA 05-0/2006, Madrid, 590 pp. (Available
515 through bibl@enresa.es)

516 Fernández, A.M., Sánchez-Ledesma, D.M., Melón, A., Robredo, L. M., Rey, J.J., Labajo
517 M.A., Clavero, M.A., Carretero, S., González A.E. 2017. Thermo-hydro-geochemical
518 behaviour of a Spanish bentonite after dismantling of the FEBEX in situ test at the
519 Grimsel Test Site. Informe Técnico CIEMAT/DMA/2G216/03/16. Madrid, 106 pp.

520 García-Siñeriz, J.L, Abós, H., Martínez, V., de la Rosa, C., Mäder, U., Kober, F. 2016.
521 FEBEX-DP: Dismantling of the heater 2 at the FEBEX "in situ" test. Description of
522 operations Nagra Arbeitsbereich NAB16-011. Wettingen, 92 pp.

523 Karnland, O., Sandén, T., Johannesson, L.E., Eriksen, T.E., Jansson, M., Wold, S., Pedersen,
524 K., Motamedi, M., Rosborg, B. 2000. Long term test of buffer material. Final report
525 on the pilot parcels. Technical Report TR-00-22, Svensk Kärnbränslehantering AB,
526 Stockholm, 131 pp.

527 Karnland O., Olsson S., Nilsson U., 2006. Mineralogy and sealing properties of various
528 bentonites and smectite-rich clay materials. SKB Technical Report TR-06-30. Svensk
529 Kärnbränslehantering AB. Stockholm, 117 pp.

530 Karnland, O., Olsson, S., Dueck, A., Birgersson, M., Pedersen, K., Nilsson, S., Eriksen, T.E.,
531 Rosborg, B. 2009. Long term test of buffer material at the Äspö Hard Rock
532 Laboratory, LOT project. Final report on the A2 test parcel. SKB Technical Report
533 TR-09-29. Svensk Kärnbränslehantering AB, Stockholm, 296 pp.

534 Karnland, O., Olsson, S., Sandén, T., Fälth, B., Jansson, M., Eriksen, T.E., Svärdström, K.,
535 Rosborg, B., Muurinen, A. 2011. Long term test of buffer material at the Äspö Hard
536 Rock Laboratory, LOT project. Final report on the A0 test parcel. SKB Technical
537 Report TR-09-31, Svensk Kärnbränslehantering AB, Stockholm, 123 pp.

538 Kharaka, Y.K., Smalley, W.C. 1976. Flow of water and solutes through compacted clays.
539 Bull. Am. Assoc. Pet. Geol. 60: 973-980. Lloret, A.; Villar, M.V.; Sánchez, M.; Gens,
540 A.; Pintado, X. & Alonso, E.E. 2003. Mechanical behaviour of heavily compacted
541 bentonite under high suction changes. *Géotechnique* 53(1): 27-40.

542 Martínez, V., Abós, H., García-Siñeriz, J.L. 2016. FEBEXe: Final Sensor Data Report
543 (FEBEX “in situ” Experiment). Nagra Arbeitsbereich NAB 16-019. Wetingen, 244
544 pp.

545 Olsen, H.W. 1962. Hydraulic flow through saturated clays. 9th Nat. Conf. On Clays and Clay
546 Minerals. Pergamon. Oxford. 170-182.

547 Olsson, S., Jensen, V., Johannesson, L.E., Hansen, E., Karnland, O., Kumpulainen, S.,
548 Kiviranta, L., Svensson, D., Hansen, S., Lindén, J. 2013. Prototype Repository.
549 Hydro-mechanical, chemical and mineralogical characterization of the buffer and
550 tunnel backfill material from the outer section of the Prototype Repository. Technical
551 Report TR-13-21, Svensk Kärnbränslehantering AB, Stockholm, 168 pp.

552 Sánchez, M.; Villar, M.V.; Lloret, A. & Gens, A. 2007. Analysis of the expansive clay
553 hydration under low hydraulic gradient. In: *Experimental Unsaturated Soil Mechanics*.
554 Springer Proceedings in Physics, vol. 112. Springer, Berlin. 309-318.

555 Svensson, D., Dueck, A., Nilsson, U., Olsson, S., Sandén, T., Lydmark, S., Jägerwall, S.,
556 Pedersen, K., Hansen, S. 2011. Alternative buffer material. Status of the ongoing

557 laboratory investigation of reference materials and test package 1. Technical Report
558 TR-11-06, Svensk Kärnbränslehantering AB, Stockholm, 146 pp.

559 Villar, M.V. 2002. Thermo-hydro-mechanical characterisation of a bentonite from Cabo de
560 Gata. A study applied to the use of bentonite as sealing material in high level
561 radioactive waste repositories. Publicación Técnica ENRESA 01/2002. 258 pp.
562 Madrid. (Available through bibl@enresa.es) Villar, M.V. (ed.) 2006. FEBEX Project
563 Final report. Post-mortem bentonite analysis. Publicación Técnica ENRESA 05-
564 1/2006. ENRESA, Madrid. 183 pp. ISSN 1134-380X. (Available through
565 bibl@enresa.es)

566 Villar, M.V. & Lloret, A. 2001. Variation of the intrinsic permeability of expansive clay upon
567 saturation. In: ADACHI, K. & FUKUE, M.(eds.): Clay Science for Engineering.
568 Balkema, Rotterdam. 259-266.

569 Villar, M.V.& Lloret, A. 2007. Dismantling of the first section of the FEBEX in situ test:
570 THM laboratory tests on the bentonite blocks retrieved. Physics and Chemistry of the
571 Earth, Parts A/B/C 32 (8-14): 716-729.

572 Villar, M.V. & Lloret, A. 2008. Influence of dry density and water content on the swelling of
573 a compacted bentonite. Applied Clay Science 39: 38-49.

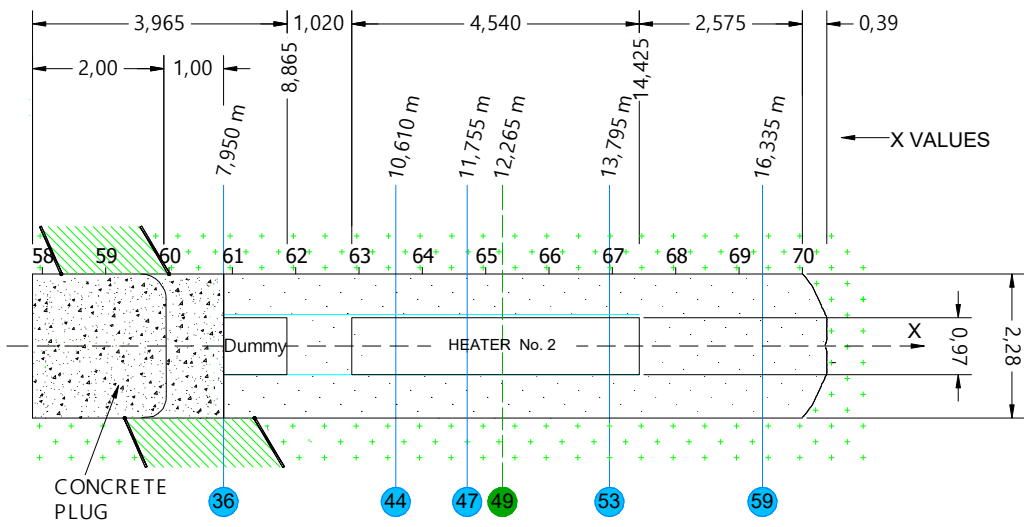
574 Villar, M.V. & Gómez-Espina, R. 2009. Report on thermo-hydro-mechanical laboratory tests
575 performed by CIEMAT on FEBEX bentonite 2004-2008. Informes Técnicos CIEMAT
576 1178. Madrid, 67 pp. Agosto 2009.

577 Villar, M.V.; Iglesias, R.J.; Abós, H.; Martínez, V.; de la Rosa, C. & Manchón, M.A. 2016a.
578 FEBEX-DP onsite analyses report. Nagra Arbeitsbereich NAB 16-012. Wettingen,
579 101 pp.

580 Villar, M.V., Gutiérrez-Rodrigo, V., Iglesias, R.J., Campos, R., Gutiérrez-Nebot, L. 2016b.
581 Changes on the microstructure of compacted bentonite caused by heating and
582 hydration. 3rd European Conference On Unsaturated Soils - E-UNSAT 2016. E3S Web
583 of Conferences 9, 18001.

584 Villar, M.V., Iglesias, R.J., Gutiérrez-Alvarez, C., Carbonell, B., Campos, R., Campos, G.,
585 Martín, P.L., Castro, B. 2018. FEBEX-DP: Thermo-hydro-mechanical postmortem
586 analysis of bentonite performed at CIEMAT. Technical report
587 CIEMAT/DMA/2G216/2/16. Nagra Arbeitsbereich NAB 16-024. Wetingen, 136 pp.

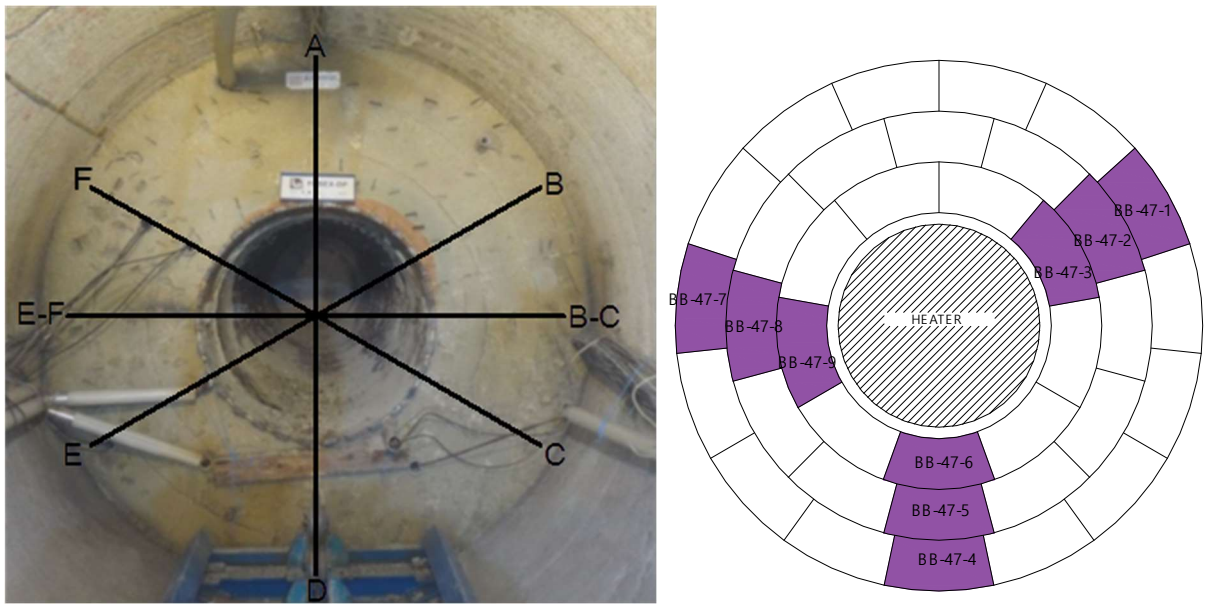
588



- 1
- 2
- 3
- 4

Figure 1: General layout of the in situ test during phase II and location of the sampling sections from which the samples sent to CIEMAT were taken (S49 was analysed on site)

5

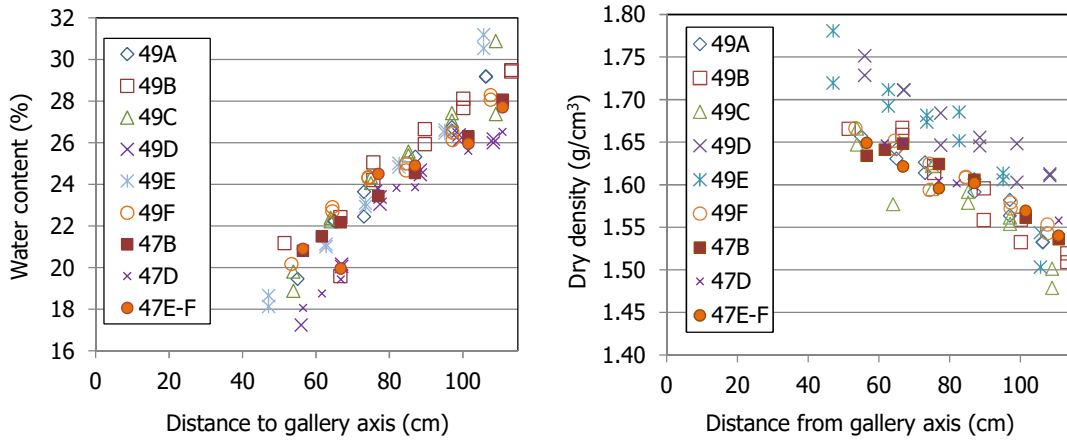


6

7 **Figure 2: Left: appearance of the bentonite barrier after extraction of heater 2 in 2015, with indication of**
8 **sampling radii; Right: location and reference of block samples from sampling section S47 sent to**
9 **CIEMAT (coloured, BB stands for Bentonite Block, 47 is the sampling section as in Figure 1)**

10

11

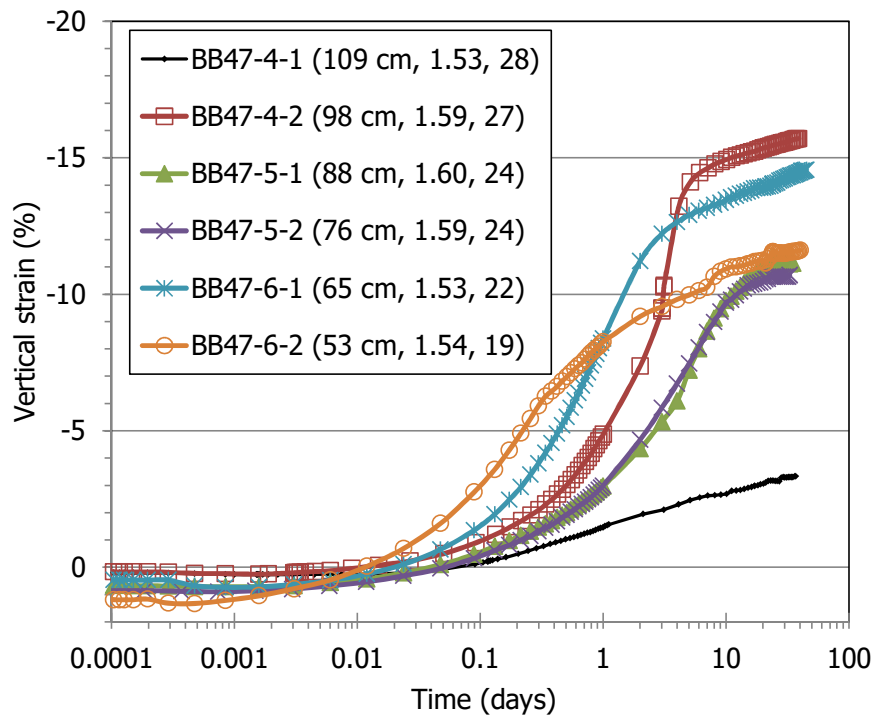


12

13 **Figure 3: Comparison of water content and dry density measured in close-by sections S47 (CIEMAT's**
14 **lab) and S49 (onsite, Villar et al. 2016a). The location of the sections is indicated in Figure 1. The letters in**
15 **the legend indicate the sampling radius according to Figure 2**

16

17



18

19

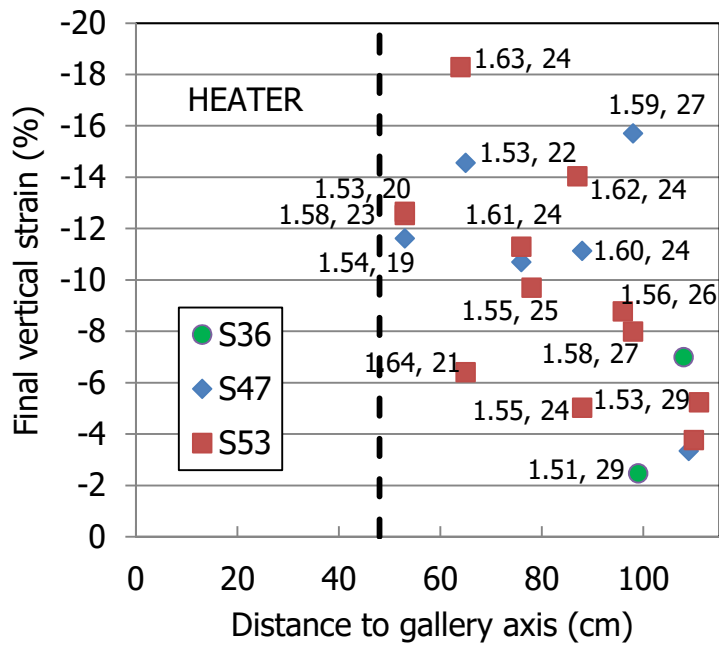
20

21

Figure 4: Evolution of vertical strain during the swelling under 0.5 MPa stress for samples of section S47. The reference of the samples corresponds to the block reference indicated in Figure 2. The distance to the axis, the dry density (g/cm^3) and water content (%) of each sample are indicated in the legend

22

23

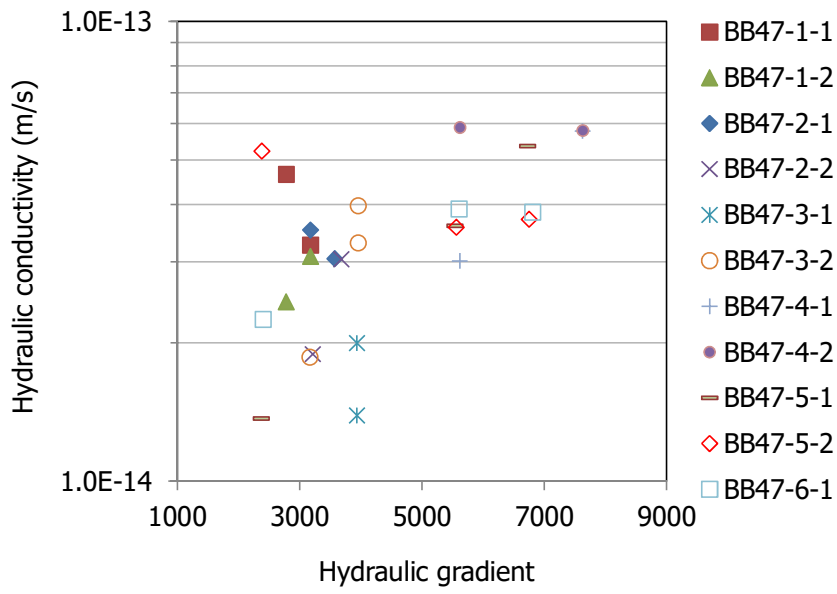


24

25 **Figure 5: Final vertical strain for samples of different sections saturated under vertical stress 0.5 MPa**
26 **(the initial dry density and water content of some of the specimens is indicated in g/cm³ and %)**

27

28

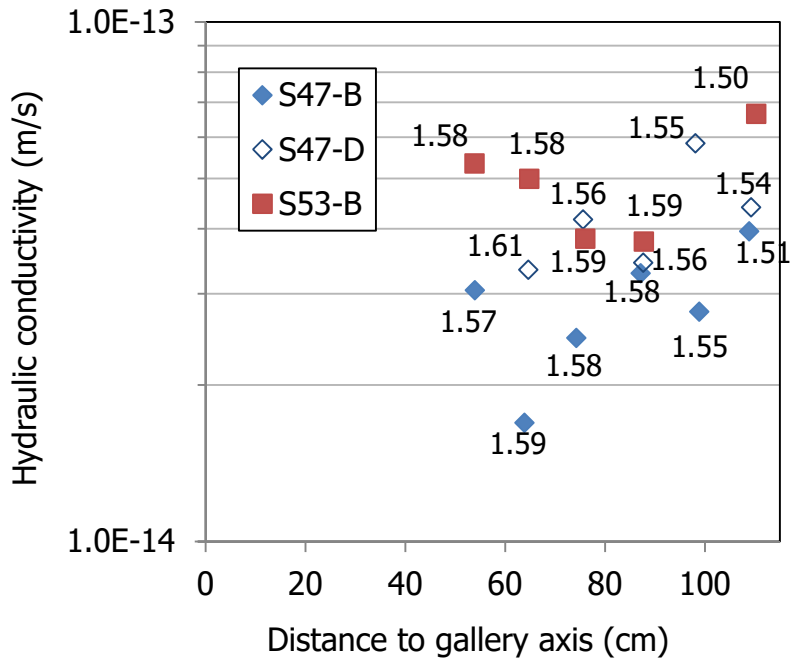


29

30 **Figure 6: Hydraulic conductivity of samples from section S47 as a function of the hydraulic gradient**
31 **applied (the references of the samples correspond to the names of the blocks indicated in Figure 2)**

32

33

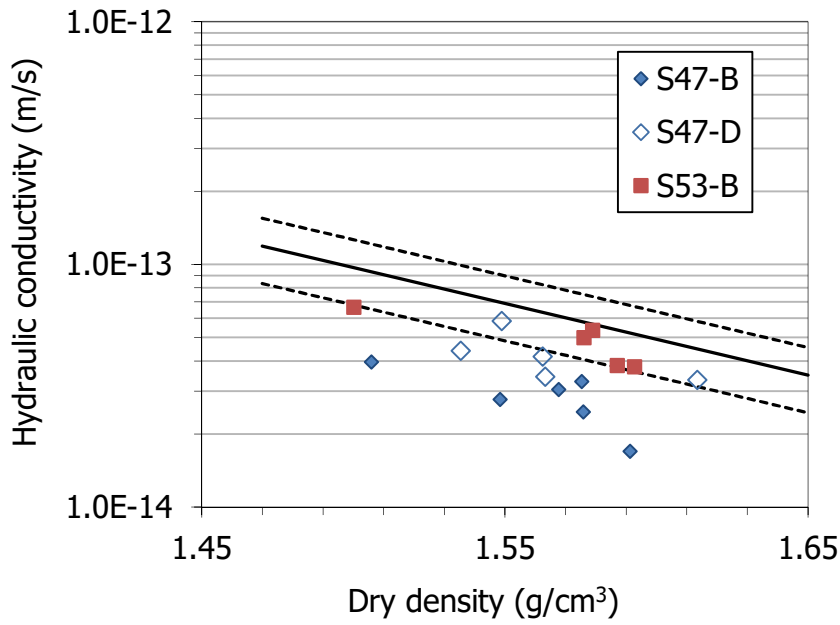


34

35 **Figure 7: Hydraulic conductivity of samples from section S47 and S53 taken along different radii (the dry**
36 **density of the specimens is indicated in g/cm³)**

37

38

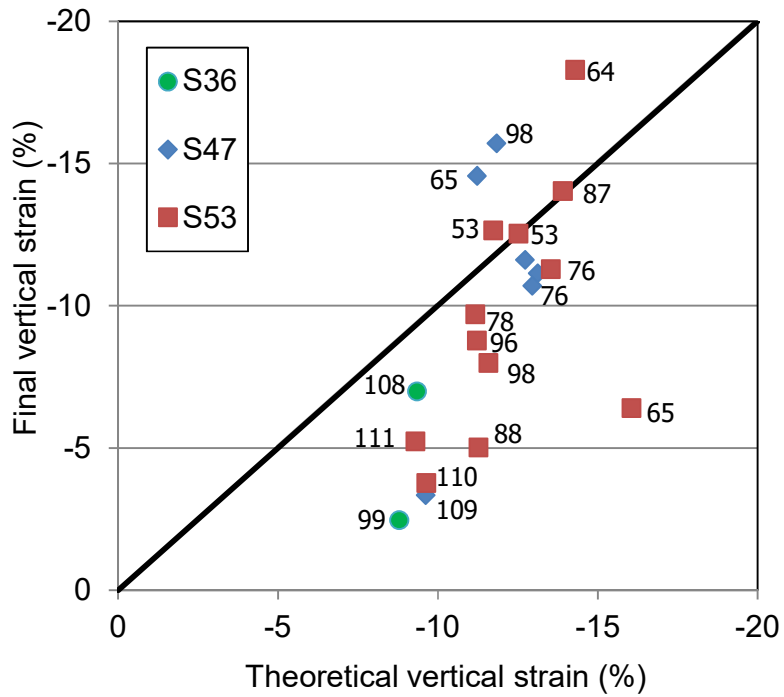


39

40 Figure 8: Hydraulic conductivity of samples from different sections and radii (indicated in the legend) and
41 empirical correlation for untreated FEBEX bentonite obtained with Eq. 2 (solid line, the dashed lines
42 indicate the expected range of variation, 30%)

43

44

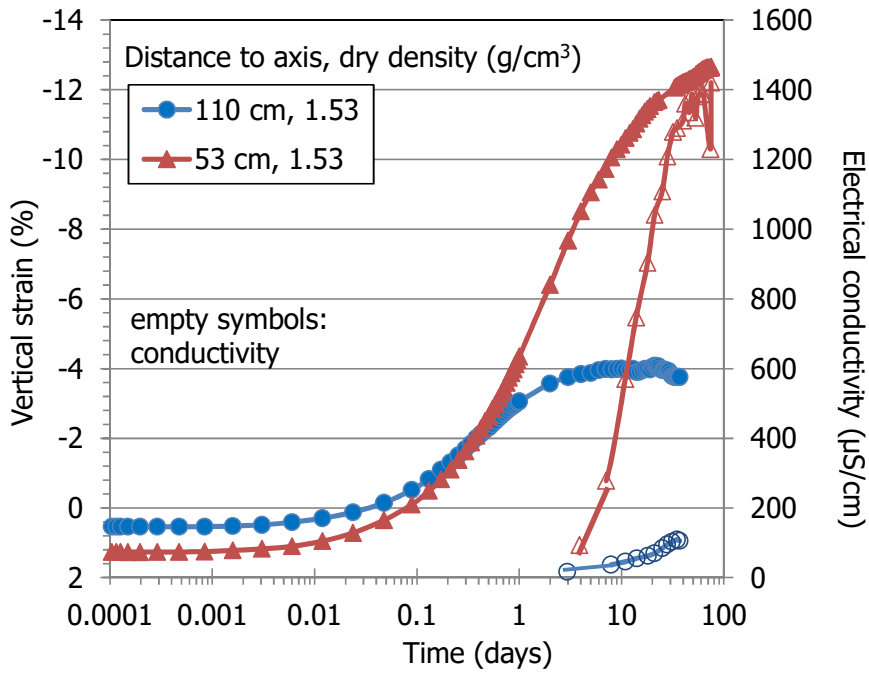


45

46 **Figure 9: Comparison between the vertical strain measured at the end of the swelling under load tests and**
47 **the strain corresponding to equivalent samples of the reference bentonite tested under the same conditions**
48 **obtained with Eq. 1. The distance to the gallery axis of each sample is indicated in cm**

49

50

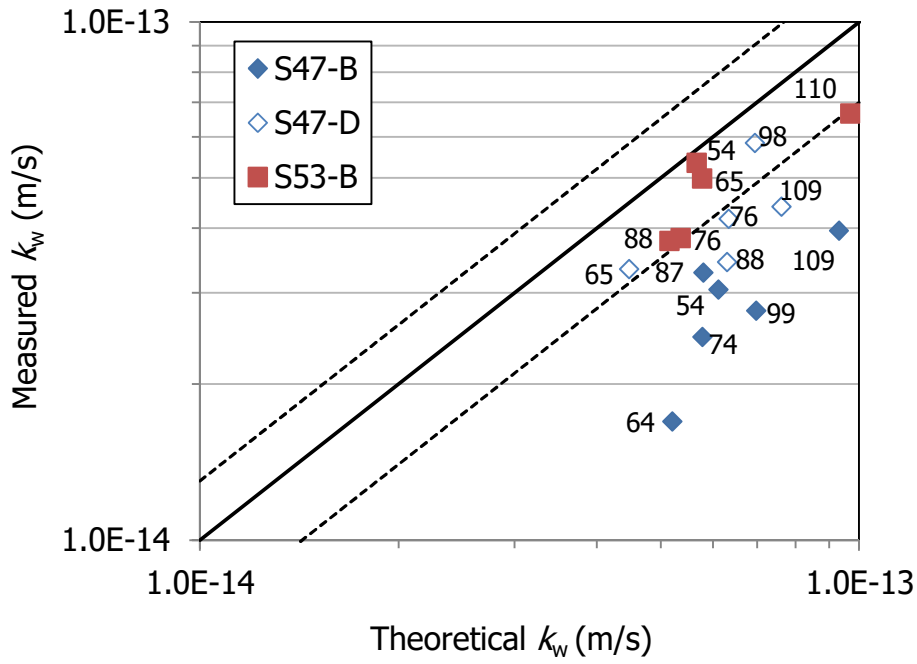


51

52 **Figure 10: Evolution of vertical strain and electrical conductivity of the water in the oedometer cell during**
53 **the swelling under 0.5 MPa vertical stress for two samples of section S53**

54

55



56

57 **Figure 11: Comparison between the hydraulic conductivity measured and that corresponding to samples**
58 **of the reference bentonite of the same dry density obtained with Eq. 2. The distance to the gallery axis of**
59 **each sample is indicated in cm**

60